

Rare Earth Elements Association with Predominant Elements in Solids Precipitated during Alkalinization of Acid Mine Water

Dilesha Jayahansani Kotte-Hewa^{1,2}, Delphine Durce¹, Sonia Salah¹, Erik Smolders²

¹Belgian Nuclear Research Centre (SCK•CEN), Expert Group Waste & Disposal, Boeretang, 2400, Mol, Belgium, dilesha.kotte.hewa@sckcen.be, ORCID 0000-0001-7757-1571

²KU Leuven, Department of Soil and Water Management, Kasteelpark Arenberg 20, 3001 Heverlee, Belgium, erik.smolders@kuleuven, ORCID 0000-0003-3054-2444

Abstract

Rare Earth Elements (REE) scavenging during remediation of acid mine water using Passive Treatment Systems (PTS) resulted in PTS to be considered as a potential source of REE. This has sparked interest in the possible retrieval of REE from the solids precipitated along PTS. The development of an efficient retrieval method requires first to assess the REE scavenging mechanisms and to identify any possible association/correlation of REE with predominant elements (i.e. Fe, Al, Mn, Ca, S) present in the precipitated solids. These first steps were here tackled using Laser Ablation (LA) Inductively Coupled Plasm-Mass Spectrometry (ICP-MS) in combination to Scanning Electron Microscope/Energy Dispersive X-ray spectroscopy (SEM/EDX). PTS was simulated by batch alkalinization experiments, which were performed to sequentially increase the pH of an acid mine water sample through CaCO₃ addition. The solids precipitated up to pH≈4 and between pH 4–6 were collected separately for characterization. Results revealed a medium positive correlation ($R^2 > 0.5$) between Ca and S in the solids collected up to pH≈4 indicating gypsum precipitation which was also confirmed by SEM/EDX. In addition, a strong positive correlation ($R^2 > 0.7$) between Ca, S and light REEs (LREEs) was observed pointing also to an association of LREEs with gypsum. In the solid collected between pH 4–6, LREEs and Gd showed strong positive correlations with Fe and medium positive correlations with Al. The observed correlations indicate that during the alkalinization of acid mine water by CaCO₃, gypsum acts as a host mineral for LREEs at low pH (up to pH≈4) while at higher pH (between pH 4–6), Fe and Al oxyhydroxides appear to be the preferential host minerals for LREEs, Gd and Er. This implies that for the possible recovery of REE from PTS, gypsum can be targeted mostly in the first layers of the PTS and especially for LREEs whereas Fe- and Al- oxyhydroxides can be targeted for all REE further on in the PTS, i.e. where higher pH are obtained.

Keywords: AMD remediation, passive treatment systems (PTS), alkalinization, REE scavenging mechanisms, laser ablation ICP-MS

Introduction

REE are crucial for the production of modern high technological devices due to their unique optical, magnetic and paramagnetic properties and thus they are considered as technology critical elements (Bau *et al.* 2018; Costis *et al.* 2021; Soyol-Erdene *et al.* 2018). Passive treatment systems (PTS) installed for the remediation of acid mine water have recently gained much attention due to their ability to scavenge Rare Earth Elements (REE)

and as such PTS are considered as a potential source of REE (Ayora *et al.* 2016; Hedin *et al.* 2019). REE include 15 Lanthanides (from La to Lu) plus Y. REE are further classified as light REE (LREE), i.e. from La to Sm, middle REE (MREE), i.e. from Eu to Dy and heavy REE (HREE), i.e. from Ho to Lu although this classification is not always consistent in the literature (Bau *et al.* 2018; Costis *et al.* 2021; Soyol-Erdene *et al.* 2018). Acid mine water remediation using PTS mostly involves use

of alkaline materials, e.g. calcite to neutralize the pH thereby leading to the precipitation of metals (Orden *et al.* 2021). Upon contact, calcite dissolution begins and is associated to the consumption of protons present in the acid mine water and thus pH gradually goes up. Along this alkalization process, at specific/characteristic pH ranges, the major constituents of the acid mine water, i.e. Fe and Al start to precipitate as secondary mineral phases. As reported in literature, Fe-bearing phases generally start to precipitate first, e.g. as iron oxyhydroxysulfates (i.e. schwertmannite) at pH between 3–4.5 and Al-comprising phases rather precipitate later at pH between 4.5–6 as e.g. Al oxyhydroxysulfates (i.e. basaluminite) (Lozano *et al.* 2019a, 2020; Sánchez-España *et al.* 2011). Related to the calcite dissolution during alkalization is the precipitation of gypsum which has been reported to occur in the acid (pH = 3) to alkaline (pH = 9) range (Lozano *et al.* 2019a, 2020; Lozano *et al.* 2019b; Sánchez-España *et al.* 2011). If present, Mn can also be precipitated (i.e. as Mn oxyhydroxysulfates, Mn oxides and Mn carbonates) at pH above 8 (Hedin *et al.* 2019). REE are also scavenged inside these PTS and are attributed mainly to being associated with Al containing mineral phases (i.e. basaluminite) (Ayora *et al.* 2016; Orden *et al.* 2021). REE scavenging along the PTS with those mineral phases has sparked interest in their possible retrieval from these solids. To develop an efficient retrieval method it is necessary to first assess the REE scavenging mechanisms and to identify any possible association/correlation of REE with predominant elements (i.e. Fe, Al, Mn, Ca, S) present in the precipitated solids. However, the presence of REE at trace level (i.e. μmol) limits the identification of such associations/correlations using conventional solid characterization techniques such as Scanning Electron Microscope/Energy Dispersive X-ray spectroscopy (SEM/EDX) or X-Ray Fluorescence Spectroscopy (XRF). Laser-Ablation (LA) Inductively Coupled Plasma-Mass Spectrometry (ICP-MS) represents a powerful tool in this regards as it simultaneously enables multi-element analysis including REE at μmol or below (Danyushevsky *et al.* 2011; Merten *et*

al. 2005). LA ICP-MS was therefore used in this study with the objective of identifying REE associations with the aforementioned predominant elements present in the solids precipitated at characteristic pH ranges.

Methods

A sample of acid mine water was collected from the Tharsis mining area in the Iberian Pyrite Belt (IPB) in southwest Spain. The pH of the water was measured to 2 and its cationic composition (major and trace elements including REE) measured by ICP-MS was as follows. Fe = 70 mmol/L, Al = 40 mmol/L, Ca = 10 mmol/L, Mn = 4 mmol/L, Zn = 7 mmol/L, Cu = 1 mmol/L, La = 2 $\mu\text{mol/L}$, Ce = 6 $\mu\text{mol/L}$, Pr = 0.8 $\mu\text{mol/L}$, Nd = 4 $\mu\text{mol/L}$, Sm = 1 $\mu\text{mol/L}$, Eu = 0.3 $\mu\text{mol/L}$, Gd = 2 $\mu\text{mol/L}$, Tb = 0.2 $\mu\text{mol/L}$, Dy = 1 $\mu\text{mol/L}$, Ho = 0.2 $\mu\text{mol/L}$, Er = 0.7 $\mu\text{mol/L}$, Tm = 0.09 $\mu\text{mol/L}$, Yb = 0.5 $\mu\text{mol/L}$ and Lu = 0.07 $\mu\text{mol/L}$. Sulfate concentration measured by IC was 400 mmol/L.

Batch alkalization experiments were performed to sequentially increase the pH of the acid mine water and to obtain solid precipitates up to pH \approx 4, as the representative pH for Fe-oxyhydroxysulfate precipitation, and solid precipitates between pH 4–6, as the representative pH for Al-oxyhydroxysulfate precipitation. Alkalization was achieved through addition of CaCO₃ to aliquots of the acid mine water sample. The required solid (CaCO₃) to liquid (acid mine water) ratio to increase pH up to pH \approx 4 was 11 g/L, and to sequentially increase the pH from 4 to 6, an additive 4 g/L was needed. The precipitated solids were separated from the supernatant by centrifugation (Sigma 6-16KS) at 7000 \times g for 10 min after a reaction time of two weeks in an orbital shaker (Ohaus Orbital Shaker) at constant speed. The solid phases were then freeze-dried and subsequently sieved with a 50 μm sieve for characterization using LA-ICP-MS and SEM/EDX. Each solid was pressed into 1.3 cm sized pellets before characterization by LA ICP-MS and by SEM/EDX. An Analyte Excite Excimer LA coupled with 8900 Triple Quadrupole ICP-MS was used to determine the correlation of selected LREE, i.e., La, Ce, Pr and Nd, the MREE, i.e. Gd and the HREE, i.e. Er with the

predominant major elements, such as Fe, Al, Mn, Ca and S. A summary of operational parameters used in the LA ICP-MS analysis is given in Table 1.

Calibration was performed using two National Institute of Standards and Technology (NIST) Standard Reference Materials (SRM), NIST SRM 610 and NIST SRM 612. To maximize the sensitivity, the LA ICP-MS operational parameters were optimized using NIST SRM 612, 1) for low laser-induced elemental fractionation based on $^{238}\text{U}/^{232}\text{Th}$ ratio (≈ 1) and 2) for low oxide formation based on $^{248}\text{ThO}/^{232}\text{Th}$ ratio ($< 2\%$). 25 spots per each solid (pellet) were analyzed for Fe, Al, Mn, Ca, S, La, Ce, Pr, Nd, Gd and Er. Each spot was ablated and measured at every 0.65 s for 30 s time period (thus ≈ 46 /spot). Before and after the analysis of each sample, the NIST 610 and NIST 612 were also ablated each at four different locations

and were measured. The average counts of each elements per spot were calculated after correcting for background signal and the correlation of REE with the other elements were determined based on correlation coefficient (R^2).

SEM/EDX (Phenom Desktop equipped with EDX) was used to observe the morphology and to identify the elemental composition of the solid phases. The pellets were mounted on aluminum stubs and coated with an ultrathin layer (5 nm) of gold to make their surfaces conductive before analysis by SEM/EDX. Imaging was done at a voltage of 10 kV, while EDX spot analyses targeting major phases were performed at an elevated voltage of 15 kV.

Results and Discussion

SEM images of formed solids up to $\text{pH}\approx 4$ and between pH 4–6 are shown in Figure 1. It is

Table 1 Summary of operational parameters used in the LA ICP-MS analysis

Parameter	Value
Spot size (μm)	40
Laser mode	Burst
Fluence (J/cm^2)	2.5
Repetition rate (Hz)	10
Shot count	300
Pre-ablation time (s) (for measuring background signal)	30
Ablation time (s)	0.65
Post-ablation time (s) (as cleaning step)	30
Waiting time between each spot analysis (s)	30

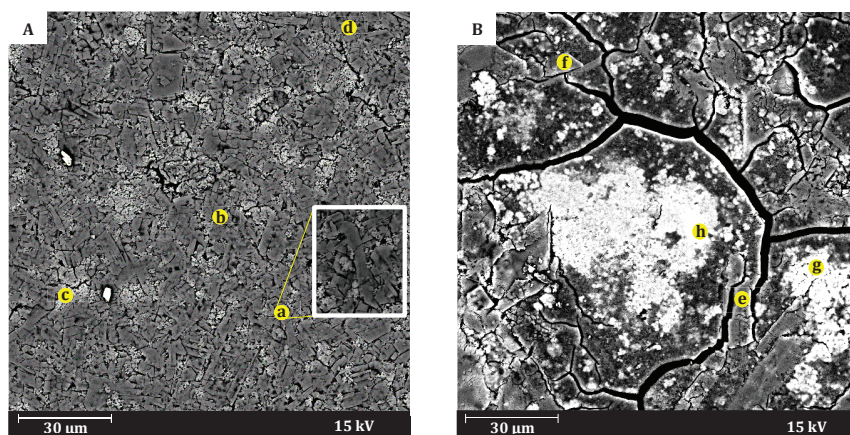


Figure 1 SEM images of formed solid samples up to $\text{pH}\approx 4$: A and between pH 4–6: B. A zoomed-in view of spot a is shown inside the white framed area.

noteworthy that at low pH (up to $\text{pH} \approx 4$), the surface is mainly covered by Ca, S and O rich phases (as revealed by EDX) corresponding to gypsum minerals with characteristic elongated shape having a length of $< 30 \mu\text{m}$ and a width of $< 10 \mu\text{m}$ (denoted by the spots of a and b). In addition, Fe, O and S rich phases (denoted by the spots of c and d) with rather amorphous morphology are also present at low pH (up to $\text{pH} \approx 4$). The latter comprise also minor amounts of Al, revealing that part of Al has been co-precipitated with the Fe mineral phases although Al mineral phase precipitation is rather favored at slightly higher pH (> 4.5).

At higher pH (between pH 4–6), comparatively wider forms of gypsum minerals (Ca, S and O rich phases) having a width of $> 10 \mu\text{m}$ could be observed (denoted by the spots of e and f) together with Al, S and O rich mineral phases (denoted by the spots of g and h). The latter are clearly amorphous which is in agreement with literature (Lozano *et al.* 2019a, 2020; Sánchez-España *et al.* 2011). Furthermore, considerable amounts of Zn and Cu are also present revealing favorable co-precipitation of those metals along with Al mineral phases. However, neither Mn nor selected REEs were detectable with SEM/EDX.

The calculated La, Ce, Pr, Nd, Gd and Er correlations (R^2) each with Fe, Al, Mn, Ca

and S b up to $\text{pH} \approx 4$ and between pH 4–6 obtained using LA ICP-MS data analysis are shown in Figure 2. Further Fe, Al, Mn and Ca correlations (R^2) each with S up to $\text{pH} \approx 4$ and between pH 4–6 obtained using LA ICP-MS data analysis are shown in Figure 3. Results revealed, regardless of the pH range, medium positive correlations ($0.4 \leq R^2 < 0.7$) between Ca and S confirming the presence of gypsum minerals in each precipitate (Figure 3) in agreement with observations made by SEM/EDX.

At low pH (up to $\text{pH} \approx 4$), LREE showed strong positive correlations ($R^2 \geq 0.7$) with Ca and S (Figure 2), indicating association of LREE with gypsum. In addition, Gd showed a medium positive correlation ($R^2 \approx 0.6$) with Ca and S, while those elements are not correlated with Er ($R^2 \approx 0$) (Figure 2). The association of LREE and gypsum can be attributed to similarities between their ionic radii and Ca^{2+} in the gypsum structure (8-fold coordination) (Ma *et al.* 2020). Results further revealed that all the selected REE are not correlated with Fe and Al at low pH (up to $\text{pH} \approx 4$) (Figure 2). Moreover, Fe and Al are also not correlated with S at this low pH (up to $\text{pH} \approx 4$) (Figure 3) showing that S concentration is mostly controlled by the gypsum precipitation even though some Fe oxyhydroxysulfate phases are expected to

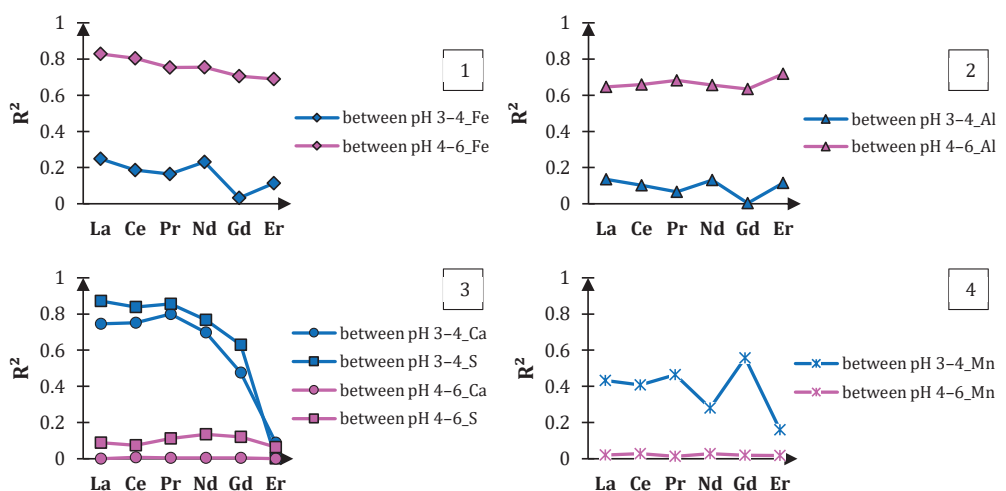


Figure 2 La, Ce, Pr, Nd, Gd and Er correlations (R^2) with 1: Fe, 2: Al, 3: Ca and S and 4: Mn up to $\text{pH} \approx 4$ (denoted by blue lines) and between pH 4–6 (denoted by pink lines) obtained using LA ICP-MS data analysis.

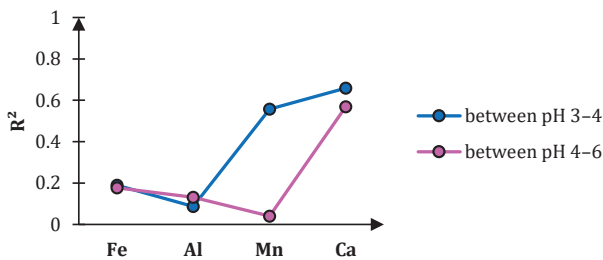


Figure 3 Fe, Al, Mn and Ca correlations (R^2) each with S up to $pH \approx 4$: A (denoted by blue lines) and between pH 4–6 (denoted by pink lines) obtained using LA ICP-MS data analysis.

precipitate. Conversely, Mn shows a medium positive correlation with S ($R^2 \approx 0.6$) (Figure 3) most likely due to co-precipitation as Mn phases precipitation is not favored at this pH. Further, La, Ce, Pr and Gd show a medium positive correlation with Mn ($0.4 \leq R^2 < 0.7$) while Nd and Er are poorly correlated with Mn ($R^2 < 0.4$).

On the contrary, at higher pH (between pH 4–6) the correlations are mostly reversed. All the selected REE show positive correlations with Fe ($R^2 \geq 0.7$) yet, it decreases from LREE to Er. With Al however, LREE and Gd reveal medium positive correlations ($0.4 \leq R^2 < 0.7$) whereas Er shows a higher positive correlation ($R^2 \approx 0.7$). However, Fe and Al correlations with S have not changed even in the higher pH range (between pH 4–6) and stay as not correlated. No correlations exist between selected REE and Ca ($R^2 \approx 0$) and also between those of and Mn ($R^2 \approx 0$). Correlation between Mn and S has changed to none.

Based on the correlations described above, it is clear that gypsum immediately gets precipitated during alkalization of acid mine water through addition of $CaCO_3$. Therefore, when gypsum precipitation predominates (i.e. at low pH up to $pH \approx 4$), LREE are co-precipitated due to the ionic radii similarity mentioned above. This implies for the possible recovery of REE from PTS, gypsum can be targeted especially for LREEs. Even beyond pH 4, the concentration of Ca^{2+} and sulfur appear to be controlled by gypsum precipitation. During the stepwise increase of pH from pH 4–6, association of REE was observed to shift from gypsum to Fe- and Al-phases. The positive correlations of REE with Fe and Al at higher pH might

be explained either by co-precipitations or sorption to respective mineral phases, but needs still to be confirmed. The fact, that no correlation was identified between Al, Fe and S (see above), suggests that instead of Fe-/Al-oxyhydroxysulfates (i.e. schwertmannite, basaluminite), rather Fe and Al oxyhydroxides could be the host minerals for REE or that the precipitation of gypsum still controls the S concentration at higher pH and screen the correlation of S with Fe/Al.

Conclusions

This study sought at investigating the association/correlation of selected LREEs, i.e. La, Ce, Pr and Nd, MREE, i.e. Gd and HREE, i.e. Er with the predominant major elements, such as Fe, Al, Mn, Ca and S present in the formed solids in AMD during the sequential increase of pH (i.e. up to $pH \approx 4$ and between pH 4–6) through the addition of $CaCO_3$. This was achieved by using LA ICP-MS complementary to SEM/EDX. It was thereby intended to identify possible scavenging mechanisms of the selected REEs in the mentioned pH ranges.

Correlations (R^2) obtained using LA ICP-MS data analysis revealed medium positive correlations ($0.5 < R^2 < 0.7$) between Ca and S up to $pH \approx 4$ and between pH 4–6 indicating gypsum precipitation, which was also confirmed by SEM/EDX. In addition, a strong positive correlation ($R^2 > 0.7$) between Ca, S and the LREEs was observed revealing association of LREEs with gypsum between pH 4–6, LREEs and Gd showed strong positive correlations with Fe ($R^2 > 0.7$) and medium positive correlations with Al ($0.5 < R^2 < 0.7$). No correlation was however

observed of the latter elements with sulfur. This suggests that at higher pH either Fe and Al oxyhydroxides to be host minerals for REE or due to S concentration being still controlled by the gypsum precipitation might have screened the correlation of S with Fe/Al. This implies that for the possible recovery of REE from PTS, gypsum can be targeted mostly in the first layers of the PTS and especially for LREEs whereas Fe- and Al- oxyhydroxides can be targeted for all REE further on in the PTS, i.e. where higher pH are obtained.

Acknowledgements

The authors want to acknowledge that this study is part of the ITN PANORAMA – This project has received funding from European Union's Horizon 2020 research and innovation program under the Marie Skłodowska-Curie Grant Agreement N°857989. The authors gratefully acknowledge the valuable assistance of the following people as well: Dr. Carlos Ruiz Cánovas and Dr. Raul Moreno Gonzalez from the Department of Earth Sciences, University of Huelva in Spain for assistance in collecting acid mine water samples; Dr. Alicia Van Ham-Meert, Dr. Charlotte Vermeiren and Mr. Jesse Dekeyrel, Division of Soil and Water management, KU Leuven for their immense assistance in measuring samples for LA ICP-MS; All the technicians, Waste and Disposal Group, SCK.CEN for their assistance in various ways.

References

- Ayora C, Macias F, Torres E, Lozano A, Carrero S, Nieto JM, Perez-Lopez R, Fernandez-Martinez A, Castillo-Michel H (2016) Recovery of Rare Earth Elements and Yttrium from Passive-Remediation Systems of Acid Mine Drainage. *Environ Sci Technol* 50(15):8255-62. <https://doi.org/10.1021/acs.est.6b02084>
- Bau M, Schmidt K, Pack A, Bendel V, Kraemer D (2018) The European Shale: An improved data set for normalisation of rare earth element and yttrium concentrations in environmental and biological samples from Europe. *Applied Geochemistry* 90:142-149. <https://doi.org/10.1016/j.apgeochem.2018.01.008>
- Costis S, Mueller KK, Coudert L, Neculita CM, Reynier N, Blais J-F (2021) Recovery potential of rare earth elements from mining and industrial residues: A review and cases studies. *Journal of Geochemical Exploration* 221. <https://doi.org/10.1016/j.gexplo.2020.106699>
- Danyushevsky L, Robinson P, Gilbert S, Norman M, Large R, McGoldrick P, Shelley M (2011) Routine quantitative multi-element analysis of sulphide minerals by laser ablation ICP-MS: Standard development and consideration of matrix effects. *Geochemistry: Exploration, Environment, Analysis* 11(1):51-60. <https://doi.org/10.1144/1467-7873/09-244>
- Hedin BC, Capo RC, Stewart BW, Hedin RS, Lopano CL, Stuckman MY (2019) The evaluation of critical rare earth element (REE) enriched treatment solids from coal mine drainage passive treatment systems. *International Journal of Coal Geology* 208:54-64. <https://doi.org/10.1016/j.coal.2019.04.007>
- Lozano A, Ayora C, Fernández-Martínez A (2019a) Sorption of rare earth elements onto basaluminite: The role of sulfate and pH. *Geochimica et Cosmochimica Acta* 258:50-62. <https://doi.org/10.1016/j.gca.2019.05.016>
- Lozano A, Ayora C, Fernández-Martínez A (2020) Sorption of rare earth elements on schwertmannite and their mobility in acid mine drainage treatments. *Applied Geochemistry* 113. <https://doi.org/10.1016/j.apgeochem.2019.104499>
- Lozano A, Fernandez-Martinez A, Ayora C, Di Tommaso D, Poulain A, Rovezzi M, Marini C (2019b) Solid and Aqueous Speciation of Yttrium in Passive Remediation Systems of Acid Mine Drainage. *Environ Sci Technol* 53(19):11153-11161. <https://doi.org/10.1021/acs.est.9b01795>
- Ma X, Gomez MA, Yuan Z, Bi R, Zhang J, Wang S, Yao S, Kersten M, Jia Y (2020) Incorporation of trace metals Cu, Zn, and Cd into gypsum: Implication on their mobility and fate in natural and anthropogenic environments. *Chemical Geology* 541. <https://doi.org/10.1016/j.chemgeo.2020.119574>
- Merten D, Geletneký J, Bergmann H, Haferburg G, Kothe E, Büchel G (2005) Rare earth element patterns: A tool for understanding processes in remediation of acid mine drainage. *Geochemistry* 65:97-114. <https://doi.org/10.1016/j.chemer.2005.06.002>
- Orden S, Macias F, Canovas CR, Nieto JM, Perez-Lopez R, Ayora C (2021) Eco-sustainable passive treatment for mine waters: Full-scale

- and long-term demonstration. *J Environ Manage* 280:111699. <https://doi.org/10.1016/j.jenvman.2020.111699>
- Sánchez-España J, Yusta I, Díez-Ercilla M (2011) Schwertmannite and hydrobasaluminite: A re-evaluation of their solubility and control on the iron and aluminium concentration in acidic pit lakes. *Applied Geochemistry* 26(9-10):1752-1774. <https://doi.org/10.1016/j.apgeochem.2011.06.020>
- Soyol-Erdene TO, Valente T, Grande JA, de la Torre ML (2018) Mineralogical controls on mobility of rare earth elements in acid mine drainage environments. *Chemosphere* 205:317-327. <https://doi.org/10.1016/j.chemosphere.2018.04.095>